The Stoichiometry of Host PrP^C Glycoforms Modulates the Efficiency of PrP^{Sc} Formation in Vitro†

Koren A. Nishina,‡ Nathan R. Deleault,‡ Sukhvir P. Mahal,§ Ilia Baskakov,|| Thorsten Luhrs,⊥ Roland Riek,⊥ and Surachai Supattapone*,‡

Department of Biochemistry, Dartmouth Medical School, Hanover, New Hampshire 03755, Department of Infectology, Scripps Florida, 5353 Parkside Drive, Jupiter, Florida 33458, Medical Biotechnology Center, University of Maryland Biotechnology Institute, Baltimore, Maryland 21201, and The Salk Institute for Biological Studies, 10010 North Torrey Pines Road, La Jolla, California 92037

Received July 28, 2006; Revised Manuscript Received September 10, 2006

ABSTRACT: A central event in the formation of infectious prions is the conformational change of a host-encoded glycoprotein, PrP^C, into a pathogenic isoform, PrP^{Sc}. However, the molecular requirements for efficient PrP conversion remain unknown. In this study, we employed the recently developed protein misfolding cyclic amplification (PMCA) and scrapie cell assay (SCA) techniques to study the role of N-linked glycosylation on prion formation in vitro. The results show that unglycosylated PrP^C molecules are required to propagate mouse RML prions, whereas diglycosylated PrP^C molecules are required to propagate hamster Sc237 prions. Furthermore, the formation of Sc237 prions is inhibited by substoichiometric levels of hamster unglycosylated PrP^C molecules. Thus, interactions between different PrP^C glycoforms appear to control the efficiency of prion formation in a species-specific manner.

Much evidence supports the "protein-only" hypothesis that conversion of a normal, host glycoprotein (PrP^C)[1] into a protease-resistant, infectious isoform (PrP^{Sc}) is the central pathogenic event in transmissible prion diseases such as Creutzfeldt-Jakob disease (CJD) in humans, bovine spongiform encephalopathy (BSE) in cattle, chronic wasting disease (CWD) in cervid species, and scrapie in ungulates (*1*, *2*). Although PrP^C is highly conserved among mammals, small differences in the PrP^C amino acid sequence appear to cause "species barriers", which manifest as reduced rates of disease transmission between different animal species (*3*, *4*). Interestingly, novel self-propagating "strains" of infectious prions with distinctive clinical and neuropathological features can arise when prions are inefficiently transmitted between different animal species and can then be faithfully maintained upon serial passage within the same animal species (*5*, *6*). Several studies have shown that prion strains are associated with PrP^{Sc} molecules that possess distinctive biochemical characteristics (*7*−*11*) and that some of these chemical properties can be propagated in vitro (*12*). Species-dependent transmission barriers and strain variation appear to be related phenomena (*13*). Recent biophysical studies of model proteins suggest that the formation of prion strains may be governed by differences in the potential folding pathways available to different protein substrates (*14*−*17*).

Mature PrP molecules possess glycans linked to asparagine residues 180 and 196 and a C-terminal glycophosphatidylinositol (GPI) anchor (*18*−*20*). The relative distribution of di-, mono-, and unglycosylated PrP^C glycoforms varies between different animal species, and regional variations in the stoichiometry of PrP^C glycoforms have also been identified within the brains of individual animals (*21*−*23*). The ability of different prion strains to maintain distinctive distributions of PrP^{Sc} glycoforms upon serial passage suggests that the N-linked glycans may play an important role in the specificity of PrP conversion (*9*). Therefore, we decided to investigate whether the glycosylation profile of PrP^C molecules influences the species and/or strain specificity of prion formation.

Other investigators previously studied this question by either (1) inhibiting glycosylation in cells using tunicamycin (*24*−*26*) or (2) expressing PrP molecules with mutant

† This work was supported by the National Institutes of Health (R21 AI058979, R01 NS046478, and T32 AI007519), the Burroughs Wellcome Fund, Pew Charitable Trusts, and the U.S. Army.

* To whom correspondence should be addressed: Department of Biochemistry, 7200 Vail Building, Dartmouth Medical School, Hanover, NH 03755. Phone: (603) 650-1192. Fax: (603) 650-1193. E-mail: supattapone@dartmouth.edu.

‡ Dartmouth Medical School.

§ Scripps Florida.

|| University of Maryland Biotechnology Institute.

⊥ The Salk Institute for Biological Studies.

[1] Abbreviations: PrP^C, cellular isoform of the prion protein; PrP^{Sc}, scrapie isoform of the prion protein; PMCA, protein misfolding cyclic amplification; SCA, scrapie cell assay; CJD, Creutzfeldt-Jakob disease; BSE, bovine spongiform encephalopathy; CWD, chronic wasting disease; GPI, glycophosphatidylinositol; PrP27−30, purified proteinase K-digested PrP^{Sc}; UN, preparation enriched for unglycosylated PrP^C; DI, preparation enriched for diglycosylated PrP^C; DI → UN, DI preparation subjected to enzymatic deglycosylation; ALL, preparation of PrP^C containing di-, mono-, and unglycosylated PrP^C; MOPS, 3-(*N*-morpholino)propanesulfonic acid; EDTA, ethylenediaminetetraacetic acid; IMAC, immobilized metal affinity chromatography; PNGase F, peptide *N*-glycosidase F; MWCO, molecular weight cutoff; WGA, wheat germ agglutinin; SP, sulfonylpropyl; Abl, 10% (w/v) ablated ($Prnp^{0/0}$) brain homogenate; PK, proteinase K; PBS, phosphate-buffered saline without calcium or magnesium; PVDF, polyvinylide difluoride; TBST, Tris-buffered saline with Tween; HRP, horseradish peroxidase; Ha, hamster; Mo, mouse; REC, *E. coli*-expressed, α-helical, recombinant PrP molecules; CFC, cell-free conversion; Tg, transgenic.

10.1021/bi061526k CCC: $33.50
Published on Web 11/03/2006

glycosylation sites in transgenic mice (*27*, *28*). However, such manipulations could potentially cause abnormal folding and/or trafficking of PrP molecules during biosynthesis (*27*, *29*−*31*), and polypeptide sequence dissimilarities between mutant and wild-type PrP^C molecules could also affect transmission barriers and strain recognition in a manner independent of glycosylation. Furthermore, pharmacologic and genetic approaches cannot be used to study possible functional interactions between different PrP^C glycoforms. Therefore, we used a direct biochemical approach to produce and isolate natively processed, wild-type PrP^C glycoforms from hamsters and mice, two related species with different native PrP^C glycoform distributions. We then used the protein misfolding cyclic amplification (PMCA) technique (*32*) to test the ability of isolated PrP^C glycoforms, alone and in combination, to amplify and propagate purified proteinase K-digested PrP^{Sc} (PrP27−30) molecules. The results of these experiments revealed unexpected functional interactions between PrP^C glycoforms, which regulate prion formation in a species-specific manner.

MATERIALS AND METHODS

Preparation of Crude Brain Homogenates. Either one hamster brain or two mouse brains (Harlan Sprague Dawley, Inc., Indianapolis, IN) were Potter homogenized in 10 mL of ice-cold PBS (phosphate-buffered saline without calcium or magnesium) containing Complete protease inhibitors (Roche, Indianapolis, IN). The homogenate was centrifuged at 200*g* for 30 s, and the postnuclear supernatant was collected.

Preparation of Native and Unglycosylated PrP^C (UN, DI → UN). We used a modified protocol to partially purify PrP^C based on the method described by Pan et al. (*33*). All steps were performed at 4 °C. Either six hamster or 12 mouse brains were Potter homogenized in 40 mL of ice-cold buffer A [20 mM MOPS (pH 7.0) and 150 mM NaCl] containing Complete EDTA-free protease inhibitors. The homogenate was initially centrifuged at 200*g* for 30 s; the postnuclear supernatant was then removed and centrifuged at 3200*g* for 20 min. The resulting pellet was resuspended and Dounce homogenized in 30 mL of buffer A and Complete EDTA-free protease inhibitors. Four milliliters of a 10% DOC/Triton X-100 detergent mixture was added to the homogenate, and the mixture was incubated on ice for 30 min and centrifuged at 100000*g* for 30 min. The solubilized supernatant was applied to a pre-equilibrated 2 mL IMAC-$CuSO_4$ column (GE Healthcare, Piscataway, NJ). The column was washed with 10 mL of IMAC-$CuSO_4$-W [buffer A, 10 mM imidazole in buffer A (pH 7.0), and 1% Triton X-100] and eluted with 10 mL of IMAC-$CuSO_4$-E1 [20 mM MES (pH 6.4), 150 mM imidazole in buffer A (pH 7.0), 150 mM NaCl, and 1% Triton X-100]. The IMAC-$CuSO_4$ eluate was applied to a pre-equilibrated 2 mL SP Sepharose cation exchange column (Sigma, St. Louis, MO). The column was washed with 10 mL of SPW [20 mM MOPS (pH 7.0), 250 mM NaCl, and 1% Triton X-100] and eluted with 8 mL of SPE [20 mM MOPS (pH 7.5), 500 mM NaCl, and 1% Triton X-100].

The N-linked glycans were removed from PrP^C using glycerol-free PNGase F (peptide *N*-glycosidase F) (New England Biolabs, Beverly, MA) under nondenaturing conditions; 50 μL of glycerol-free PNGase F (∼25000 units) was added to 500 μL of SP eluate, and the mixture was incubated for 24 h at 37 °C. After the initial incubation, an additional 50 μL of PNGase F was added, and the mixture was incubated for an additional 24 h at 37 °C. The sample was repurified using a pre-equilibrated 200 μL IMAC-$CuSO_4$ resin; all subsequent steps were performed at 4 °C. Initially, the sample was incubated on an end-over-end rotator with the IMAC-$CuSO_4$ slurry for 30 min in a capped column support (Bio-Rad, Hercules, CA). The column was then washed with 20 mL of IMAC-$CuSO_4$-W and eluted with 500 μL of IMAC-$CuSO_4$-E1. The eluate was loaded into a 3500 MWCO Slide-A-Lyser (Pierce, Rockford, IL) and dialyzed overnight into buffer C [20 mM MOPS (pH 7.5), 150 mM NaCl, and 0.5% Triton X-100] to yield the deglycosylated PrP^C product "UN". The "Native" sample used in Figure 1A was incubated with PBS instead of PNGase F but otherwise processed identically.

To generate "DI → UN", 50 μL of "DI" (prepared as described below) was incubated with 5 μL of PNGase F (2500 units) for 24 h at 37 °C.

Preparation of Glycosylated PrP^C (ALL, DI). A solubilized supernatant from either mouse or hamster brain homogenate was obtained as described in the preceding section. This solubilized supernatant was first applied to a pre-equilibrated 2 mL IMAC-$CuSO_4$ column. The column was washed with 10 mL of IMAC-$CuSO_4$-W and eluted with 4 mL of IMAC-$CuSO_4$-E2 [20 mM MOPS (pH 7.5), 750 mM NaCl, 150 mM imidazole in buffer A (pH 7.0), and 1% Triton X-100]. This eluate was then applied to a pre-equilibrated 1 mL WGA (wheat germ agglutinin) (Vector Laboratories, Burlingame, CA) column. The flow-through fraction was collected and dialyzed overnight into buffer C to yield a preparation of PrP^C containing all three glycoforms in an approximately equal distribution (ALL).

Meanwhile, the WGA column was washed with 20 mL of WGAW1 [20 mM MOPS (pH 7.5), 750 mM NaCl, and 1% Triton X-100], followed by 5 mL of WGAW2 [20 mM MOPS (pH 7.5), 150 mM NaCl, and 1% Triton X-100]. The sample was eluted with 4 mL of WGAE (buffer B, 50 mM *N*-acetylglucosamine, and 1% Triton X-100) and dialyzed overnight into buffer C to yield the diglycosylated PrP^C substrate (DI).

Preparation of PrP27−30. PrP27−30 was prepared separately from eight different scrapie strains [five mouse strains (RML, 22A, 139A, C506, and Me7) and three hamster strains (Sc237, 139H, and Drowsy)] kindly provided by S. B. Prusiner (San Francisco, CA). Each scrapie-infected brain was homogenized in 10 volumes (w/v) of PBS with a disposable plastic homogenizer (Kendall, Mansfield, MA) and centrifuged at 200*g* for 30 s. One hundred microliters of postnuclear supernatant was diluted into 900 μL of buffer D (PBS and 1% Triton X-100) and then incubated with 10 μg/mL PK (proteinase K, specific activity of 30 units/mL) (Roche Applied Science, Mannheim, Germany) for 30 min at 20 °C. Protease digestion was terminated by the addition of 5 mM PMSF (phenylmethanesulfonyl fluoride, from a 0.3 M stock solution in methanol). The digested sample was centrifuged at 4 °C for 1 h at 100000*g*, and the pellet was resuspended in 200 μL of ice-cold buffer D by two 30 s pulses of an indirect sonicator set at output 6.5 [Misonix (Farmingdale, NY) 3000-MPD sonicator with a microplate horn]. An additional 800 μL of ice-cold buffer D was added

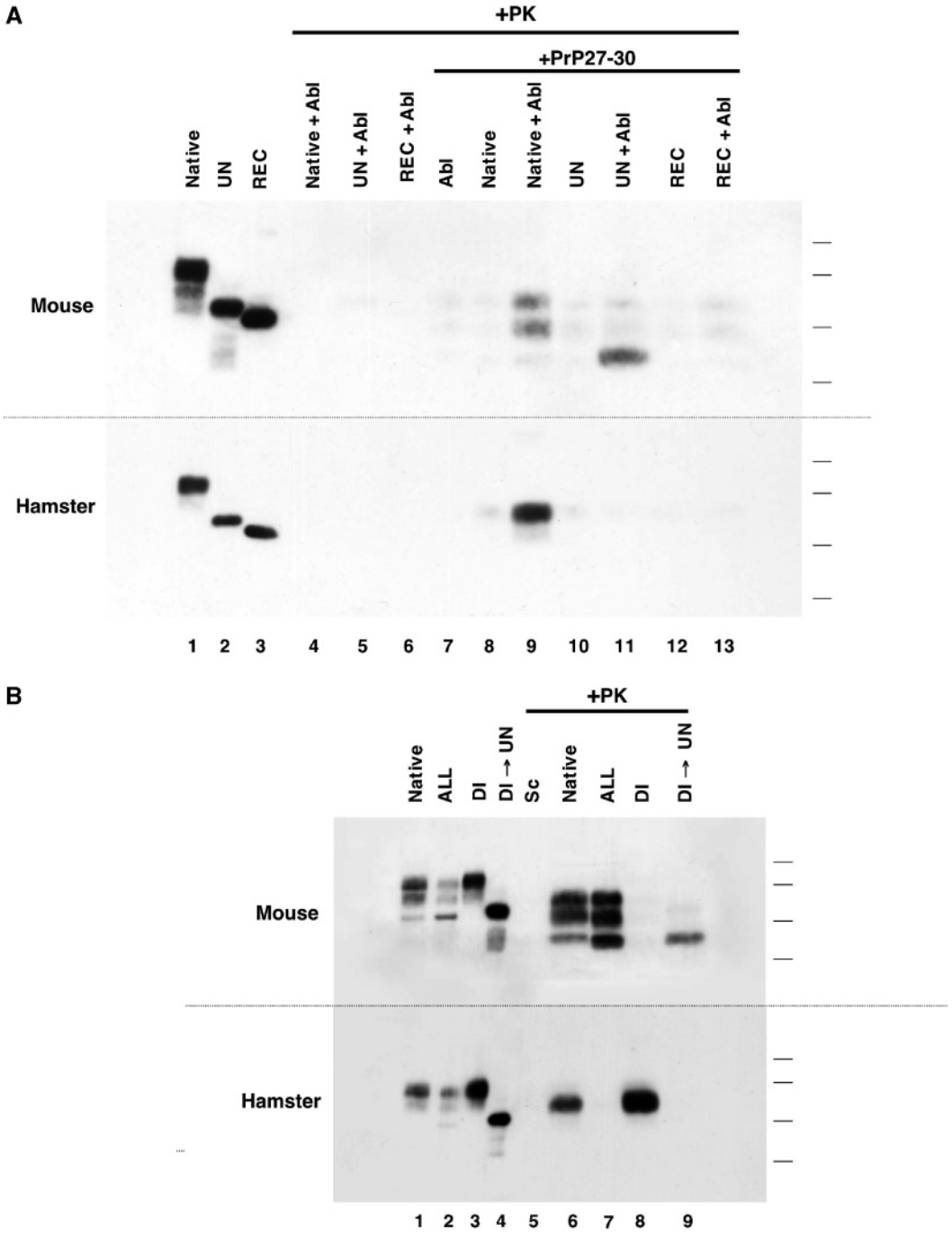

FIGURE 1: Strain-dependent conversion of various PrP substrates. (A) Western blot of PMCA reactions. Lanes 1−3 contained input substrates not treated with protease; in lanes 4−12, each of the indicated substrates was subjected to PMCA in the absence (lanes 4−6) or presence (lanes 7−12) of PrP27−30 template. Labels: Native, native PrP^C; UN, unglycosylated PrP^C; REC, recombinant PrP23−231; Abl, $Prnp^{0/0}$ brain homogenate. (B) Western blot of PMCA reactions. Lanes 1−4 contained input samples not treated with protease; in lanes 5−9, each of the indicated substrates was subjected to PMCA with PrP27−30 template in the presence of 2.5% Abl brain homogenate. Labels: ALL, flow-though fraction of lectin column; DI→UN, unglycosylated PrP^C prepared by deglycosylation of the DI preparation; +PK, digested with proteinase K; Sc, negative control reaction mixture lacking PrP^C substrate; Mouse, mouse substrates and RML template; Hamster, hamster substrates and Sc237 template. The apparent molecular mass markers on all Western blots are at 40, 33, 24, and 17 kDa. Similar results were obtained in three independent experiments.

to the suspension, and the sample was then centrifuged for 30 min at 100000*g* and 4 °C. The resulting pellets (with the exception of 22A) were resuspended in 1 mL of buffer D as described above. RML, 139A, Sc237, 139H, and Drowsy were used in the amplification reaction at a 1:10 dilution; Me7 and C506 were used in the amplification reaction at a 1:20 dilution. 22A was resuspended in 100 μL of buffer D by sonication and was used in the amplification reaction with no dilution.

Protein Misfolding Cyclic Amplification (PMCA). PMCA was performed by the method of Castilla et al. (*34*) using the various PrP^C substrate preparations described in preceding sections. The total 111 μL amplification reaction volume was composed of 50 μL of PrP^C substrate, 25 μL of Abl [10% (w/v) $Prnp^{0/0}$ brain homogenate], 1 μL of 500 mM EDTA (pH 8.0), 10 μL of 500 mM imidazole in buffer A (pH 7.0), 0.75% Triton X-100, and 25 μL of PrP27−30 (diluted as described above). When present, recombinant PrP23−321

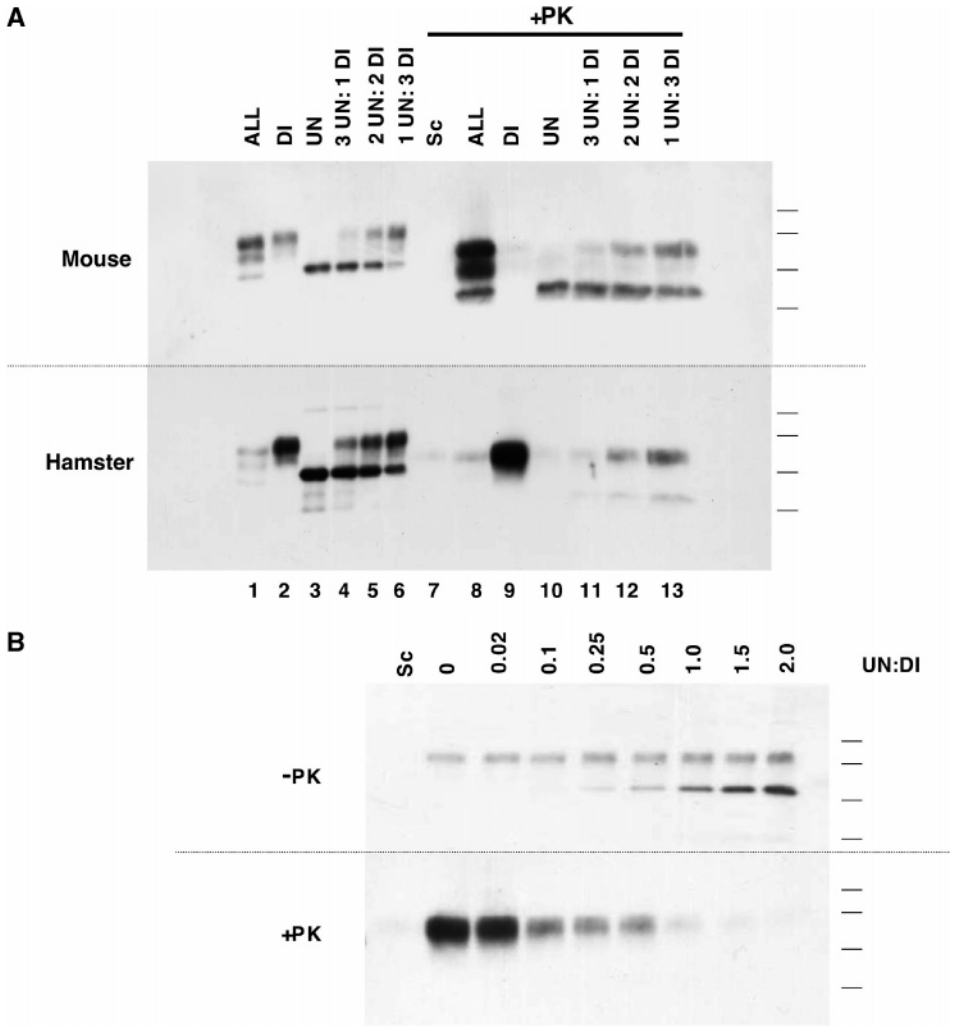

FIGURE 2: Functional interactions between PrP^C glycoforms. (A) PMCA reactions using mixtures of PrP^C substrates. Each of the indicated substrates was subjected to PMCA with PrP27−30 template in the presence of 2.5% Abl brain homogenate. Abbreviations: Sc, no PrP^C substrate added; ALL, flow-though fraction of the lectin column; 3UN:1DI, 37.5 μL of UN and 12.5 μL of DI added to the PMCA reaction mixture; 2UN:2DI, 25 μL of UN and 25 μL of DI; 1UN:3DI, 12.5 μL of UN and 37.5 μL of DI. (B) PMCA reactions using a fixed concentration of diglycosylated hamster PrP^C and varying concentrations of unglycosylated hamster PrP^C. Each of the indicated substrates was subjected to PMCA with Sc237 PrP27−30 template in the presence of 2.5% Abl brain homogenate. All samples contained 20 μL of DI $HaPrP^C$ and varying amounts of UN $HaPrP^C$. Labels: UN:DI, molar ratio of UN $HaPrP^C$ to DI $HaPrP^C$ in the substrate mixture; +PK, digested with proteinase K; Sc, negative control reaction mixture lacking PrP^C substrate. Similar results were obtained in three independent experiments. Using Adobe Photoshop to quantitate signal intensities, and assuming molecular masses of 27 and 36 kDa for UN and DI $HaPrP^C$, respectively, we estimate that the 2UN:2DI samples have molar ratios of ~2.3 for mouse and ~0.8 for hamster.

was expressed and refolded by two independent methods as previously described (*35*, *36*) and used at a final concentration of 4 μg/mL, similar to the concentration of brain-derived PrP^C substrates used in the reactions. Reactions without ablated brain homogenate had PBS substituted for Abl. The mixtures were subjected to PMCA for 24 h using a Misonix programmable sonicator equipped with a microplate horn containing 350 mL of water, and set for 30 s bursts every 30 min at output 6.5. The temperature was maintained by circulating heated water through a section of aluminum coil to heat the air inside the acoustic chamber (Misonix), and the microplate horn was covered with a sheet of plastic film to minimize evaporation. Before each burst, the bath temperature measured 41 °C, and after each burst, the temperature measured 42 °C. Samples were mounted in a holder that prevented lid opening and held the bottom of the PCR tubes ~3 mm from the horn surface. In Figure 2, a small aliquot of each sample was removed following incubation and boiled for 10 min in an equal volume of 2× SDS sample buffer, and 10 μL of the resulting minus (−) PK samples was loaded for electrophoresis. In Figures 1 and 3A,B and Table S1 (Supporting Information), input substrate preparations were diluted 1:10 into PBS and boiled for 10 min in an equal volume of 2× SDS sample buffer, and 20 μL of each resulting minus (−) PK sample was loaded for electrophoresis. Meanwhile, the plus (+) PK samples were treated with 25 μg/mL PK and incubated for 30 min at 37 °C. The digested samples were then boiled in 2× SDS sample buffer, and 80 μL of each sample was loaded for electrophoresis.

Serial in Vitro PrP^{Sc} Propagation Reactions and Cell Infection. Serial in vitro PrP^{Sc} propagation reactions were performed by the method of Castilla et al. (*34*) using the PrP^C preparations described above. The initial (day 1) reaction mixture was composed of 100 μL of PrP^C, 50 μL of 10% (w/v) Abl, 2 μL of 500 mM EDTA (pH 8.0), 20 μL of 500 mM imidazole in buffer A (pH 7.0), 0.75% Triton X-100, and 50 μL of PrP27−30 (diluted as described above).

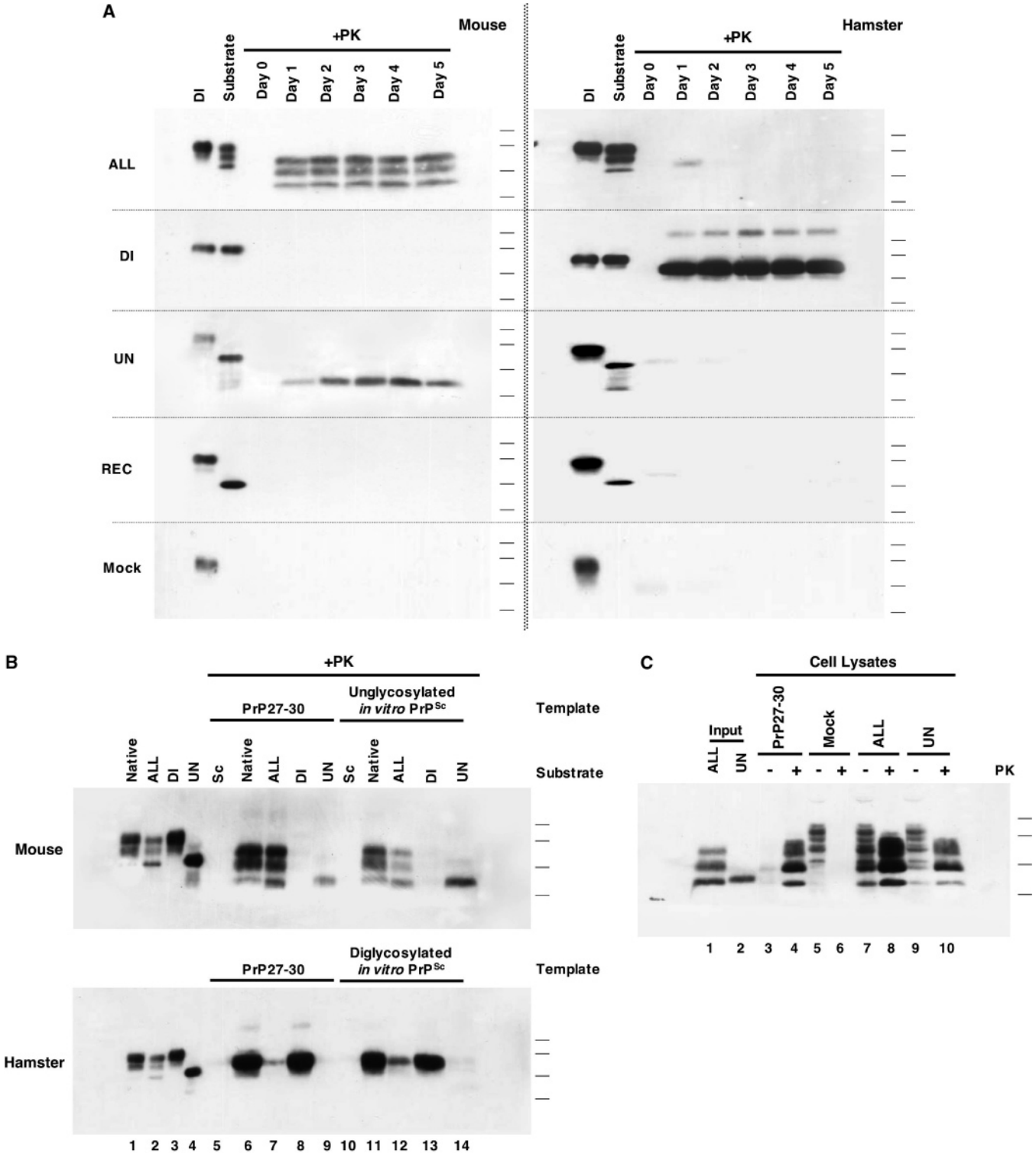

FIGURE 3: Generation and characterization of selectively glycosylated PrP^{Sc} molecules. (A) Serial propagation of PrP^{Sc} molecules in vitro. The indicated substrates were used to propagate prions in vitro for 5 days as described in Materials and Methods. In lane 1, diglycosylated PrP^{C} not subjected to protease is shown for size reference; in lane 2 is shown the input substrate used for propagation not subjected to protease, and in lanes 3−8 are shown aliquots taken after each round of PMCA treated with protease. Label: Mock, Sc237 template mock propagated without PrP^{C} substrate. (B) Seeding specificity of in vitro-generated unglycosylated RML and diglycosylated Sc237 PrP^{Sc}. Each PrP^{Sc} template was used to seed various PrP^{C} substrates, as indicated. Lanes 1−4 contained input substrates not subjected to protease; lanes 5−9 contained substrates subjected to PMCA with brain-derived PrP27−30 template, and lanes 10−14 contained substrates subjected to PMCA with in vitro-generated PrP^{Sc} templates. (C) Western blot of cell lysates infected with serially propagated, in vitro-generated PrP^{Sc} molecules. Lanes 1 and 2 contained protease-digested, in vitro-generated PrP^{Sc} inocula; lanes 3−10 contained cell lysates of N2aPK1 cells infected with indicated inocula. Labels: PrP27−30, brain-derived PrP27−30 template; Sc, negative control sample containing no PrP^{C} substrate.

The mixtures were subjected to one round of PMCA for 24 h as described above. Half of the reaction mixture (day 1) was PK digested as described above. Twenty microliters from the completed reaction (day 1) was used to seed the next 200 μL reaction mixture (day 2) containing a fresh substrate mixture [100 μL of PrP^{C}, 50 μL of 10% (w/v) Abl, 2 μL of

500 mM EDTA (pH 8.0), 20 μL of 500 mM imidazole in buffer A (pH 7.0), 8 μL of PBS, and 0.75% Triton X-100]. This process was repeated for a total of 6 days to complete six propagation rounds. Every 2 days, the bath water was changed to prevent accumulation of residue in the sonicator horn.

The final (day 6) samples were titrated between 10^{-4} and 10^{-6} using OptiMeM (Invitrogen, Carlsbad, CA), 10% bovine growth serum (Hyclone, Logan, UT), and 1% penicillin/streptomycin as a diluent and applied to highly infectable PK1 neuroblastoma cells (*37*). Following 5 × 1:8 splits, cell infectivity was measured by assaying 20 000 cells/sample, as previously described using the scrapie cell assay in end-point titration format (*37*). Wells were considered positive if the "spot" count was greater than the average background (three spots) value plus 5 times the standard deviation (six spots), i.e., ≥32 spots. The average number of infectious particles (m) in each sample was calculated using the Poisson formula $P(o) = e - m$, where $P(o)$ is the probability that a well is not infected, i.e., $P(o)$ = noninfected wells/total wells. Therefore, m = ln(total wells/noninfected wells). In parallel, infected cells were assayed for PrP^C and PrP^{Sc} content as follows. For each sample, a confluent 10 cm plate was washed with 2 × 5 mL of PBS, lysed with 2 mL of ice-cold lysis buffer [50 mM Tris (pH 8.0), 150 mM NaCl, 0.5% sodium deoxycholate, and 0.5% Triton X-100], and centrifuged briefly (<5 s) to remove debris. SDS sample loading buffer (2×) was added to a 100 μL aliquot of the supernatant and the mixture was boiled for 10 min, and 2 μL of each sample was loaded for electrophoresis of the minus (−) PK sample. Meanwhile, for plus (+) PK samples, 900 μL of the supernatant was treated with 20 μg/mL PK for 30 min at 37 °C. PK digestion was stopped with the addition of 5 mM Pefabloc (Roche), and the mixture was concentrated by centrifugation for 1 h at 100000*g* and 4 °C. The resulting pellet was resuspended in 100 μL of lysis buffer, and 2× SDS sample loading buffer was added. The sample was boiled for 10 min, and 50 μL of each sample was loaded for electrophoresis.

Electrophoresis and Immunoblotting. SDS−PAGE was performed on 1.5 mm 12% acrylamide gels with an acrylamide:bisacrylamide ratio of 29:1. Following electrophoresis, the proteins were transferred to a methanol-charged, buffer-equilibrated polyvinylide difluoride (PVDF) membrane (Millipore Corp., Bedford, MA) using a Trans-blot SD Semi-Dry Transfer Cell (Bio-Rad) set at 2 mA/cm^2 for 35 min. The membrane was treated with 3 M GdnSCN (Roche) for 30 min. Then, the membrane was rinsed with TBST [10 mM Tris (pH 7.2), 150 mM NaCl, and 0.1% Tween 20] and blocked for 1 h in skim milk (Hood, Chelsea, MA) with TBST. The blocked membrane was incubated overnight at 4 °C with 3F4 mAb diluted 1:5000 in TBST (Signet Laboratories, Inc., Dedham, MA) for detection of hamster PrP or D13-humanized Fab diluted 1:3000 in TBST (kindly provided by S. B. Prusiner) for detection of mouse PrP. Following this incubation, the membrane was washed for 3 × 10 min in TBST and then incubated for 1 h at 4 °C with either a HRP (horseradish peroxidase)-labeled anti-mouse IgG secondary antibody conjugate (diluted 1:5000 in TBST) (GE Healthcare) for 3F4 or a HRP-labeled anti-human Fab2 conjugate (diluted 1:30000 in TBST) (Pierce) for D13. The membrane was washed again for 4 × 10 min with TBST; the blot was developed with ECL reagent (Pierce), sealed in plastic covers, and exposed to Super RX film (Fujifilm, Tokyo, Japan). Exposed films were developed automatically in a Kodak M35A X-Omat film processor. Relative molecular masses of 40, 33, 24, and 17 kDa are based on migration of prestained standards (Fermentas, Hanover, MA) and are indicated at the right of each panel. Where indicated, quantitative densitometry was performed on nonsaturated film exposures using Adobe Photoshop.

RESULTS

Conversion of Specific PrP^C Glycoforms into PrP^{Sc} in Vitro. We performed reconstituted PMCA reactions by mixing various PrP^C-containing preparations, PrP^{Sc}, and crude $Prnp^{0/0}$ (Abl) brain homogenate, which provides essential cellular cofactors for the formation of both mouse and hamster PrP^{Sc} molecules in vitro (*38*) and in vivo (*3*). Using Cu^{2+} affinity and ion exchange chromatography, we partially purified PrP^C ~50-fold from either mouse (Mo) or hamster (Ha) brains to produce a native preparation of the normal distribution of PrP^C glycoforms in whole brain for each species (Figure 1A, lane 1). Because the reconstituted reaction mixtures contain crude Abl brain homogenate, we reasoned that it was not necessary for the purposes of this study to purify PrP^C to homogeneity. As expected, in the presence of Abl brain homogenate, the native preparation of $MoPrP^C$ successfully amplified PrP^{Sc} molecules derived from RML ~4-fold, and the native preparation of $HaPrP^C$, which contains little mono- or unglycosylated PrP^C, amplified PrP^{Sc} molecules from Sc237 ~12-fold (Figure 1A, lanes 7−9). We also produced an unglycosylated PrP^C substrate, designated UN, by enzymatically deglycosylating the purified, native PrP^C preparation with *N*-glycosidase F (PNGase F) under nondenaturing conditions and then repurifying the digested product (to remove the PNGase F prior to addition of Abl brain homogenate) (Figure 1A, lane 2). In PMCA reactions, the unglycosylated $MoPrP^C$ substrate successfully amplified the RML PrP^{Sc} template in the presence of Abl brain homogenate (Figure 1A, top panel, lane 11), indicating that N-linked glycosylation of PrP^C is not required for RML prion conversion. In contrast, the unglycosylated $HaPrP^C$ substrate did not amplify Sc237 PrP^{Sc} template under similar conditions (Figure 1A, bottom panel, lane 11). This unexpected result indicates that the ability of unglycosylated PrP^C molecules to undergo prion conversion is either species- or strain-dependent. *Escherichia coli*-expressed, α-helical, recombinant PrP molecules (REC) lacking post-translational modifications did not form protease-resistant PrP^{Sc} products when mixed with either RML or Sc237 prions and subjected to PMCA in the presence of Abl brain homogenate (Figure 1A, lanes 12 and 13). It is unclear why bacterially expressed PrP is not an efficient PMCA substrate, but its inefficiency may be due to either the lack of a GPI anchor or a subtle difference in protein structure compared to native PrP^C.

Next, we sought to test the ability of other PrP^C glycoforms, either alone or in combination, to convert into PrP^{Sc} by PMCA in the presence of Abl brain homogenate. To prepare PrP^C substrates with various glycoform profiles, we applied the native PrP^C preparation of each species to an immobilized lectin column in the presence of 0.75 M NaCl. The flow-through fraction of the lectin column, designated "ALL", was relatively depleted of diglycosylated and

enriched in unglycosylated PrP^C molecules, compared to the native PrP^C preparations (Figure 1B, lane 2). Subsequent elution of the column with *N*-acetylglucosamine yielded a preparation of predominantly diglycosylated PrP^C molecules, which we termed DI (Figure 1B, lane 3). We then used PNGase F to deglycosylate the DI sample, producing an unglycosylated PrP^C preparation directly derived from DI, which we termed "DI→UN" (Figure 1B, lane 4). Remarkably, isolated DI $MoPrP^C$ substrate failed to amplify the RML PrP^{Sc} template (Figure 1B, top panel, lane 8), but deglycosylation of this preparation rescued the ability of DI→UN $MoPrP^C$ substrate to convert into RML PrP^{Sc}, which indicates that the procedure used to prepare DI $MoPrP^C$ did not generate or isolate an intrinsically inactive substrate (Figure 1B, top panel, lane 9). The inability of the DI $MoPrP^C$ preparation to amplify RML PrP^{Sc} template indicates that the presence of unglycosylated $MoPrP^C$ molecules within the native $MoPrP^C$ preparation is required for conversion of the glycosylated isoforms. This surprising conclusion was confirmed by the observation that the ALL substrate containing all three $MoPrP^C$ glycoforms successfully formed RML PrP^{Sc}, including an isoform corresponding to diglycosylated PrP^{Sc} (Figure 1B, top panel, lane 7). In marked contrast, isolated diglycosylated $HaPrP^C$ substrate successfully amplified Sc237 PrP^{Sc} template, showing that the presence of unglycosylated $HaPrP^C$ molecules is not required for Sc237 PrP^{Sc} amplification (Figure 1B, bottom panel, lane 8). Furthermore, the ALL substrate containing all three $HaPrP^C$ glycoforms, including unglycosylated $HaPrP^C$, did not amplify the Sc237 PrP^{Sc} template efficiently, suggesting that unglycosylated $HaPrP^C$ molecules might competitively inhibit Sc237-induced conversion of glycosylated $HaPrP^C$ molecules (Figure 1B, bottom panel, lane 7).

Functional Interactions between PrP^C Glycoforms Regulate PrP^{Sc} Formation. Our results led us to hypothesize that the stoichiometric composition of PrP^C glycoforms controls the conversion efficiency of prion conversion and that species- and/or strain-specific interactions between different PrP^C glycoforms could modulate PrP^{Sc} formation. To test this hypothesis directly, we mixed isolated diglycosylated and unglycosylated PrP^C molecules together at various stoichiometric ratios and then tested the ability of these mixtures to serve as substrates in PMCA reactions. These reconstitution experiments confirmed that unglycosylated $MoPrP^C$ molecules are required for amplification of RML PrP^{Sc} template; even a 1:3 UN:DI molar ratio was sufficient to drive formation of both PrP^{Sc} glycoforms (Figure 2A, top panel, compare lanes 9 and 13). This result also provides additional evidence that our protocol for preparing DI $MoPrP^C$ did not create or isolate an intrinsically inactive substrate. In contrast, diglycosylated $HaPrP^C$ molecules were required for the amplification of Sc237 PrP^{Sc} template. An approximately equimolar ratio of UN to DI $HaPrP^C$ molecules was required for formation of Sc237 PrP^{Sc} in vitro (Figure 2A, bottom panel, lane 12). Paradoxically, increasing levels of unglycosylated $HaPrP^{Sc}$ could be detected as the UN:DI ratio was decreased, indicating that diglycosylated $HaPrP^C$ molecules are capable of recruiting small amounts of unglycosylated $HaPrP^C$ molecules into Sc237 prions (Figure 2A, bottom panel, lanes 12 and 13). At the same time, the presence of substoichiometric levels of unglycosylated $HaPrP^C$ appeared to inhibit the formation of Sc237 $HaPrP^{Sc}$ (Figure 2A, bottom panel, compare lanes 9 and 13). The inhibition of $HaPrP^{Sc}$ formation by unglycosylated $HaPrP^C$ in reconstituted reaction mixtures containing diglycosylated $HaPrP^C$ (Figure 2A, bottom panel, lanes 11−13 vs lane 9) supports our hypothesis that the poor conversion of the hamster ALL substrate (Figure 2A, bottom panel, compare lanes 8 and 9) is most likely caused by unglycosylated $HaPrP^C$ in the ALL substrate acting as a competitive inhibitor. To investigate the isolated effect of unglycosylated $HaPrP^C$ molecules on the formation of Sc237 PrP^{Sc} molecules, we performed an experiment in which a fixed concentration of diglycosylated $HaPrP^C$ substrate was mixed with increasing concentrations of unglycosylated $HaPrP^C$. These results confirmed that unglycosylated $HaPrP^C$ molecules potently inhibited the formation of diglycosylated Sc237 PrP^{Sc} molecules in a dose-dependent manner, even at substoichiometric ratios (Figure 2B). Furthermore, this reconstitution experiment suggests that the inability of the hamster ALL substrate to form Sc237 PrP^{Sc} molecules cannot simply be attributed to selective enrichment of an incompetent diglycosylated $HaPrP^C$ subspecies during lectin chromatography, since even competent DI $HaPrP^C$ substrate can be inhibited by addition of unglycosylated $HaPrP^C$.

The PrP^{Sc} Glycoform Profile Does Not Affect Conversion Specificity. Having established that the stoichiometry of PrP^C glycoforms in the substrate mixture regulates the efficiency of PrP^{Sc} formation in a species- and/or strain-specific manner, we next sought to examine whether the glycosylation state of PrP^{Sc} molecules in the template might also influence the specificity of PrP^{Sc} formation. To perform such experiments, it was first necessary to obtain isolated PrP^{Sc} glycoforms. To do this, we used a serial propagation protocol described by Castilla et al. (*34*) to generate isolated RML and Sc237 PrP^{Sc} glycoforms in vitro. Briefly, specific PrP^C substrates were initially mixed with PrP27−30 PrP^{Sc} template and Abl brain homogenates and subjected to PMCA for 24 h. Following this incubation, one-tenth of the reaction volume was then used to seed a new sample containing fresh PrP^C substrate and Abl brain homogenate. This process was repeated for five rounds, and samples from each round were assayed for PrP^{Sc}. The results show that unglycosylated RML PrP^{Sc} and diglycosylated Sc237 PrP^{Sc} molecules were successfully generated and propagated in vitro (Figure 3A). As expected, the ALL preparation of $HaPrP^C$ [which contains a higher proportion of the inhibitory unglycosylated glycoform compared to native brain homogenate and which does not amplify Sc237 PrP^{Sc} (Figure 1B, bottom panel, lane 7)] did not serially propagate Sc237 prions, whereas the ALL preparation of $MoPrP^C$ successfully propagated RML prions (Figure 3A, top panels). An additional sample, "Mock", was prepared in which input PrP27−30 was mock propagated without substrate (Figure 3A, bottom panels) for use in subsequent PMCA and cell culture infection assays as a negative control to confirm that six rounds of serial propagation sufficiently diluted out the original PrP27−30 input template.

We then used these novel PrP^{Sc} molecules formed by serial propagation to test whether isolated PrP^{Sc} glycoforms retained the templating characteristics of the native prion strains from which they were derived. To do so, we performed PMCA reactions using various PrP^C preparations as substrates with either brain-derived PrP27−30 or specific PrP^{Sc} glycoforms

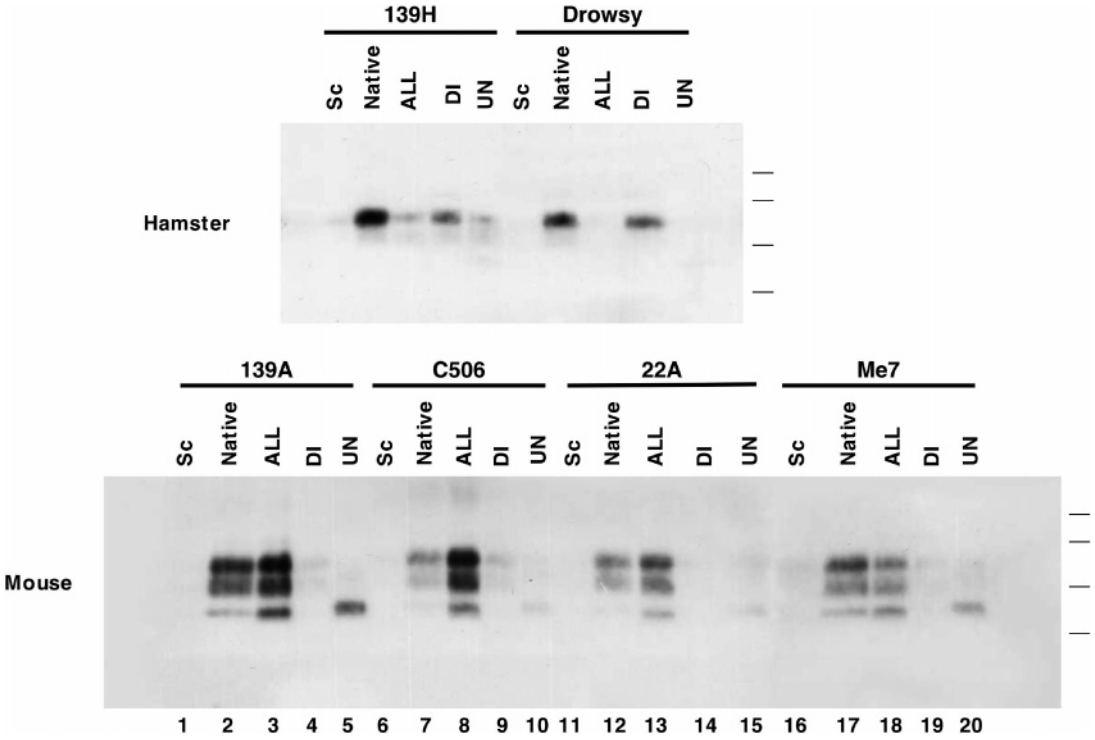

FIGURE 4: Seeding specificity of various scrapie strains. PrP27−30 template prepared from two hamster strains (139H and Drowsy) and four mouse strains (139A, C506, 22A, and Me7) were separately incubated with different preparations of PrP^C (Native, ALL, DI, and UN) and subjected to PMCA in the presence of 2.5% Abl brain homogenate, as described in Materials and Methods. All samples were subjected to proteinase K digestion. Label: Sc, negative control sample containing no PrP^C substrate. Note that the characteristic difference in electrophoretic mobility between proteinase K-digested 139H and Drowsy PrP^{Sc} molecules cannot be easily appreciated in this blot because a short gel was used, and the samples were not deglycosylated prior to electrophoresis.

as templates. The results of this comparison show that both unglycosylated RML PrP^{Sc} and diglycosylated Sc237 PrP^{Sc} templates induced the prion conversion of various PrP^C substrates in a manner indistinguishable from that of the native RML and Sc237 PrP27−30 templates, respectively (Figure 3B). Parallel reactions seeded with the negative control sample Mock showed no PrP^{Sc} formation, confirming that our in vitro-generated PrP^{Sc} templates were not contaminated with the original input PrP27−30 (data not shown). To confirm these in vitro findings, we infected cultured N2a PK1 cells with samples of in vitro-propagated RML prions containing either all three glycoforms (propagated ALL) or only unglycosylated (propagated UN) PrP^{Sc} molecules (*37*). Using the scrapie cell assay (SCA) in end-point titration format, we first confirmed that the propagated ALL and UN samples were infectious, while the Mock propagation control sample contained no detectable infectivity at the dilutions that were assayed. Specifically, these measurements indicated that the propagated ALL sample contained 4.6×10^6 infectious particles/mL, the UN sample contained 6×10^5 infectious particles/mL, and the Mock sample contained $<10^3$ infectious particles/mL (Table S1 of the Supporting Information). These results confirmed that (1) $5 \times$ 10-fold serial dilutions were adequate to reduce input infectivity to a level below detection by SCA and (*2*) unglycosylated $MoPrP^C$ is a competent substrate for forming infectious prions as well as PrP^{Sc}. When analyzed by Western blot, lysates of N2a cells infected with only unglycosylated PrP^{Sc} molecules were found to contain all three PrP^{Sc} glycoforms (Figure 3C, lane 10), confirming the results of the PMCA assays (Figure 3B, top panel, lane 11). As expected, no PrP^{Sc} was detected in cells infected with the Mock propagation control sample (Figure 3C, lane 6). Taken together, the results of our experiments with isolated PrP^{Sc} glycoforms indicate that the minimal and essential PrP entity of RML prions is unglycosylated MoPrP, which has the ability to recruit mono- and diglycosylated MoPrP molecules (Figure 3B, top panel, lanes 11 and 12, and Figure 3C, lane 10). In contrast, Sc237 prions consist mainly of diglycosylated HaPrP molecules, which are unable to recruit un- or monoglycosylated HaPrP isoforms efficiently (Figure 3B, bottom panel, lane 12).

Effects of PrP^C Sequence on the Formation of Isolated PrP^{Sc} Glycoforms. The different glycoform preferences observed in hamster versus mouse PMCA reactions could theoretically be due to either (1) differences in amino acid sequence between $HaPrP^C$ and $MoPrP^C$ molecules or (2) the different strain-specific templating properties of Sc237 versus RML prions. To distinguish between these two possibilities, we assessed the conversion of specific $HaPrP^C$ and $MoPrP^C$ glycoforms in PMCA reactions driven by other hamster and mouse prion strains. The results show that two additional strains of hamster prions successfully converted DI $HaPrP^C$, but not UN $HaPrP^C$ (Figure 4, top panel). Four additional strains of mouse prions did not convert DI $MoPrP^C$, and two of these strains successfully converted UN PrP^C (Figure 4, bottom panel). Taken together, these results suggest that the PrP sequence is the dominant factor in determining the preferred PrP^C glycoform substrate. However, the relatively poor ability of mouse prion strains C506 and 22A to convert UN PrP^C substrate suggests that strain properties of the PrP^{Sc} template may also influence PrP^C glycoform preference (Figure 4, bottom panel, compare lanes 10 and 15 to lane 5).

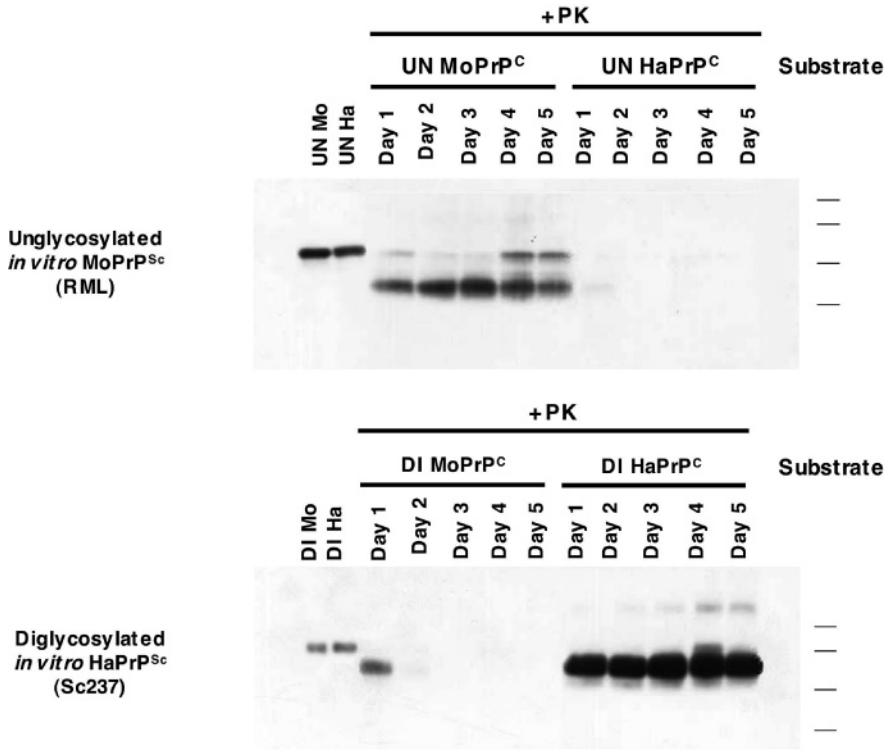

FIGURE 5: Sequence-dependent propagation barriers between isolated hamster and mouse PrP glycoforms. In vitro-generated PrP^{Sc} molecules were serially propagated for 5 days using isolated PrP^{C} glycoform substrates. For the top panel, unglycosylated RML was used as the initial seed for either unglycosylated mouse or hamster PrP^{C} substrate, as indicated. In the bottom panel, diglycosylated Sc237 was used as the initial seed for either diglycosylated mouse or hamster PrP^{C} substrate, as indicated.

The transmission of infectious prions between mice and hamsters is inefficient, and this species barrier is recapitulated in cell-free PrP^{Sc} formation assays (*39*). Previous transgenic mouse studies have established that amino acid sequence similarity between PrP^{C} and PrP^{Sc} molecules is the most important factor in determining species-dependent transmission barriers (*3*, *4*). However, since the glycoform profiles of PrP^{C} molecules differ significantly between hamsters and mice (native $HaPrP^{C}$ is relatively enriched with diglycosylated PrP^{C}), we investigated whether differential PrP glycosylation might also contribute to the transmission barrier between these two species. Using PMCA, we tested whether DI $MoPrP^{C}$ and UN $HaPrP^{C}$ substrates could propagate DI Sc237 PrP^{Sc} and UN RML PrP^{Sc} templates, respectively. The results showed that no PrP^{Sc} propagation was detected with either of these cross-species substrate−template combinations, whereas intraspecies control samples produced successful PrP^{Sc} propagation (Figure 5). Thus, PrP^{C} glycosylation does not appear to contribute significantly to species barriers in vitro.

DISCUSSION

In summary, our biochemical and cell culture studies indicate that subtle changes in the stoichiometry of host PrP^{C} glycoforms can significantly impact prion conversion in a species- and strain-specific manner. In particular, our experiments show that a substoichiometric ratio of unglycosylated $MoPrP^{C}$ molecules within a substrate mixture is required for the formation of RML prions. In contrast, diglycosylated $HaPrP^{C}$ molecules are required for, while unglycosylated $HaPrP^{C}$ molecules inhibit, the formation of Sc237 prions. The following hypothetical model could account for these results. Assuming that prions consist of a multimeric complex of PrP^{Sc} molecules (*40*), the intermolecular interaction between HaPrP molecules in the assembly of Sc237 prions may be stabilized by N-linked glycans. The assembly process would therefore require the presence of glycosylated HaPrP molecules, and binding of unglycosylated HaPrP molecules would interfere with this process (Figure 6). In contrast, N-linked glycans may cause steric hindrance for the assembly of PrP^{Sc} molecules in RML prions, and an orderly arrangement of different MoPrP glycoforms may be required to assemble this prion strain (Figure 6). Potentially, our data could also be explained by a model in which the substrate for prion propagation is a multimeric PrP^{C} complex composed of different glycoforms, and the conversion of the entire complex into PrP^{Sc} is initiated by the conversion of a specific glycoform. This alternative model would provide a simple explanation for the interesting observation that alteration of the PrP^{C} glycoform profile changes the glycoform ratio of the PrP^{Sc} molecules produced by prion-infected, cultured cells treated with tunicamycin (*26*). However, no heterogeneous, multimeric PrP^{C} complexes have yet been identified.

Because the PrP^{C} amino acid sequence is highly conserved between mice and hamsters, it is somewhat surprising that PMCA reactions using PrP molecules isolated from these two animals species should exhibit different glycoform requirements. However, recent folding studies show that recombinant HaPrP and MoPrP form amyloid fibers with different morphologies in vitro, apparently via different mechanisms of lateral assembly (*41*).

Previous studies have clearly demonstrated that radiolabeled unglycosylated $HaPrP^{C}$ substrate could convert into a protease-resistant conformation when incubated with a stoichiometric excess of Sc237 PrP^{Sc} molecules in the cell-free

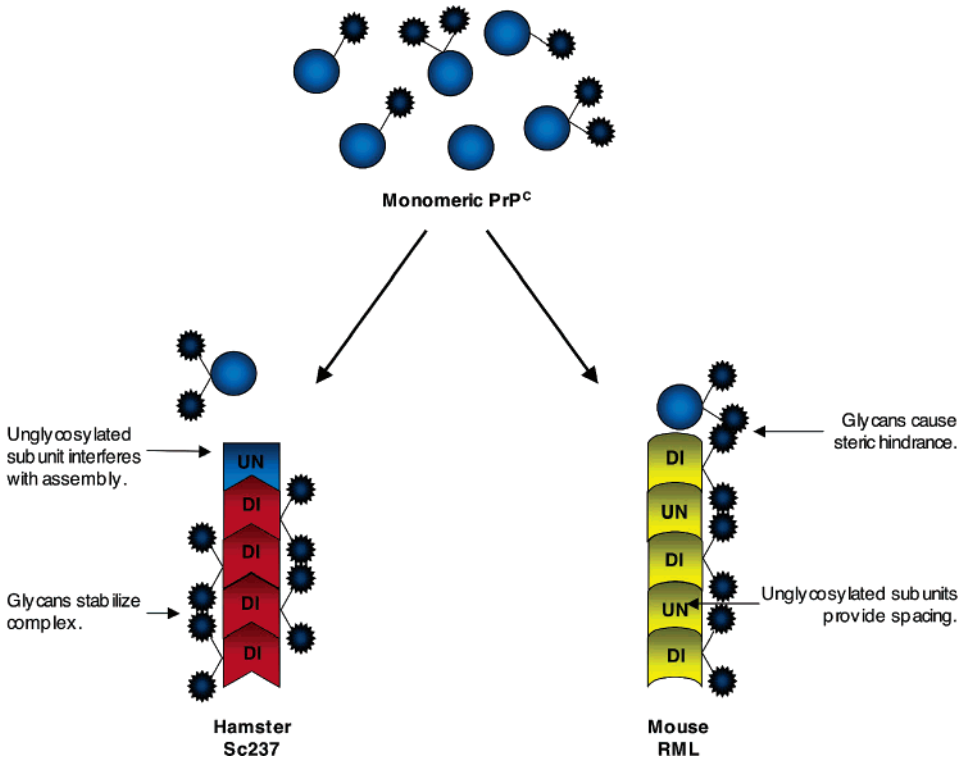

FIGURE 6: Hypothetical model of prion propagation. N-Linked glycans form crucial intermolecular contact sites between PrP monomers during Sc237 assembly but cause steric hindrance during RML assembly.

conversion (CFC) assay (*24*, *42*). The model shown in Figure 6 also provides a reasonable explanation for those findings. Although addition of unglycosylated HaPrP to Sc237 prions may inhibit elongation by "capping", this process would not necessarily prevent conversion of substoichiometric amounts of unglycosylated HaPrP caps into a protease-resistant conformation. Protease-resistant HaPrP molecules formed in this way could be specifically detected in the CFC assay because only newly converted radioactive PrP^{Sc} molecules and not template PrP^{Sc} molecules would produce autoradiographic signals. In contrast, no higher-magnitude Western blot PrP^{Sc} signals would be expected in PMCA reactions using unglycosylated $HaPrP^{C}$, since capping would inhibit PrP^{Sc} amplification.

The conclusions drawn from our biochemical experiments are consistent with infectivity studies using transgenic mice expressing selectively glycosylated $MoPrP^{C}$ molecules that appear to traffic properly to the cell surface. Those studies showed that diglycosylated $MoPrP^{C}$ is not essential for the formation of infectious prions in vivo (*28*). Our conclusions are also consistent with studies showing that Tg(HaPrP) transgenic mice coexpressing endogenous $MoPrP^{C}$ and wild-type $HaPrP^{C}$ are susceptible to Sc237 prions, because the 13A5 mAb-reactive $HaPrP^{C}$ glycoform profile of Tg(HaPrP) mice is enriched for diglycosylated $HaPrP^{C}$ in a manner similar to that of hamster brain (*3*). Unfortunately, no infectivity studies using transgenic mice expressing selectively glycosylated $HaPrP^{C}$ molecules have yet been reported.

While the data reported here provide evidence that the composition of di-, mono-, and unglycosylated PrP^{C} molecules within substrate mixtures regulates the efficiency of prion formation, an even greater level of substrate diversity could conceivably be generated by subtle variations in the architecture of the branching oligosaccharide moieties attached to individual PrP^{C} molecules (*43*). The proposed model, which includes the process of molecular selection (i.e., distinct PrP glycoforms), and the data presented also rationalize the species- and strain-specific patterns of PrP^{Sc} glycosylation (*9*), which are maintained upon serial passage. Finally, neurons in different brain regions express different, characteristic ratios of PrP^{C} glycoforms (*21*−*23*); therefore, it is reasonable to hypothesize that individual prion strains preferentially infect cells from specific brain regions because only those cells contain the appropriate PrP^{C} glycoform stoichiometry required for assembly of specifically organized aggregates of PrP^{Sc} molecules.

ACKNOWLEDGMENT

We thank Dr. Judy Rees for help editing the manuscript and Dr. Charles Weissmann for helpful discussions.

SUPPORTING INFORMATION AVAILABLE

End-point titration of prion infectivity in samples subjected to serial PMCA propagation. This material is available free of charge via the Internet at http://pubs.acs.org.

REFERENCES

1. Prusiner, S. B. (1982) Novel proteinaceous infectious particles cause scrapie, *Science 216*, 136−44.
2. Prusiner, S. B. (2000) *Prion biology and diseases*, Cold Spring Harbor Laboratory Press, Plainview, NY.
3. Scott, M., Foster, D., Mirenda, C., Serban, D., Coufal, F., Walchli, M., Torchia, M., Groth, D., Carlson, G., DeArmond, S. J., et al. (1989) Transgenic mice expressing hamster prion protein produce species-specific scrapie infectivity and amyloid plaques, *Cell 59*, 847−57.
4. Scott, M., Groth, D., Foster, D., Torchia, M., Yang, S. L., DeArmond, S. J., and Prusiner, S. B. (1993) Propagation of prions with artificial properties in transgenic mice expressing chimeric PrP genes, *Cell 73*, 979−88.

5. Bruce, M. E. (1993) Scrapie strain variation and mutation, *Br. Med. Bull. 49*, 822−38.
6. Carlson, G. A. (1996) Prion strains, *Curr. Top. Microbiol. Immunol. 207*, 35−47.
7. Bessen, R. A., and Marsh, R. F. (1992) Biochemical and physical properties of the prion protein from two strains of the transmissible mink encephalopathy agent, *J. Virol. 66*, 2096−101.
8. Telling, G. C., Parchi, P., DeArmond, S. J., Cortelli, P., Montagna, P., Gabizon, R., Mastrianni, J., Lugaresi, E., Gambetti, P., and Prusiner, S. B. (1996) Evidence for the conformation of the pathologic isoform of the prion protein enciphering and propagating prion diversity, *Science 274*, 2079−82.
9. Collinge, J., Sidle, K. C., Meads, J., Ironside, J., and Hill, A. F. (1996) Molecular analysis of prion strain variation and the aetiology of 'new variant' CJD, *Nature 383*, 685−90.
10. Peretz, D., Scott, M. R., Groth, D., Williamson, R. A., Burton, D. R., Cohen, F. E., and Prusiner, S. B. (2001) Strain-specified relative conformational stability of the scrapie prion protein, *Protein Sci. 10*, 854−63.
11. Safar, J., Wille, H., Itri, V., Groth, D., Serban, H., Torchia, M., Cohen, F. E., and Prusiner, S. B. (1998) Eight prion strains have PrP(Sc) molecules with different conformations, *Nat. Med. 4*, 1157−65.
12. Bessen, R. A., Kocisko, D. A., Raymond, G. J., Nandan, S., Lansbury, P. T., and Caughey, B. (1995) Non-genetic propagation of strain-specific properties of scrapie prion protein, *Nature 375*, 698−700.
13. Ridley, R. M., and Baker, H. F. (1996) To what extent is strain variation evidence for an independent genome in the agent of the transmissible spongiform encephalopathies? *Neurodegeneration 5*, 219−31.
14. Tanaka, M., Chien, P., Naber, N., Cooke, R., and Weissman, J. S. (2004) Conformational variations in an infectious protein determine prion strain differences, *Nature 428*, 323−8 (see comment).
15. Tanaka, M., Chien, P., Yonekura, K., and Weissman, J. S. (2005) Mechanism of cross-species prion transmission: An infectious conformation compatible with two highly divergent yeast prion proteins, *Cell 121*, 49−62.
16. King, C. Y., and Diaz-Avalos, R. (2004) Protein-only transmission of three yeast prion strains, *Nature 428*, 319−23.
17. Jones, E. M., and Surewicz, W. K. (2005) Fibril conformation as the basis of species- and strain-dependent seeding specificity of mammalian prion amyloids, *Cell 121*, 63−72.
18. Endo, T., Groth, D., Prusiner, S. B., and Kobata, A. (1989) Diversity of oligosaccharide structures linked to asparagines of the scrapie prion protein, *Biochemistry 28*, 8380−8.
19. Locht, C., Chesebro, B., Race, R., and Keith, J. M. (1986) Molecular cloning and complete sequence of prion protein cDNA from mouse brain infected with the scrapie agent, *Proc. Natl. Acad. Sci. U.S.A. 83*, 6372−6.
20. Stahl, N., Borchelt, D. R., Hsiao, K., and Prusiner, S. B. (1987) Scrapie prion protein contains a phosphatidylinositol glycolipid, *Cell 51*, 229−40.
21. DeArmond, S. J., Qiu, Y., Sanchez, H., Spilman, P. R., Ninchak-Casey, A., Alonso, D., and Daggett, V. (1999) PrPc glycoform heterogeneity as a function of brain region: Implications for selective targeting of neurons by prion strains, *J. Neuropathol. Exp. Neurol. 58*, 1000−9.
22. Beringue, V., Mallinson, G., Kaisar, M., Tayebi, M., Sattar, Z., Jackson, G., Anstee, D., Collinge, J., and Hawke, S. (2003) Regional heterogeneity of cellular prion protein isoforms in the mouse brain, *Brain 126*, 2065−73.
23. Somerville, R. A., Hamilton, S., and Fernie, K. (2005) Transmissible spongiform encephalopathy strain, PrP genotype and brain region all affect the degree of glycosylation of PrPSc, *J. Gen. Virol. 86*, 241−6.
24. Kocisko, D. A., Come, J. H., Priola, S. A., Chesebro, B., Raymond, G. J., Lansbury, P. T., and Caughey, B. (1994) Cell-free formation of protease-resistant prion protein, *Nature 370*, 471−4.
25. Taraboulos, A., Rogers, M., Borchelt, D. R., McKinley, M. P., Scott, M., Serban, D., and Prusiner, S. B. (1990) Acquisition of protease resistance by prion proteins in scrapie-infected cells does not require asparagine-linked glycosylation, *Proc. Natl. Acad. Sci. U.S.A. 87*, 8262−6.
26. Vorberg, I., and Priola, S. A. (2002) Molecular basis of scrapie strain glycoform variation, *J. Biol. Chem. 277*, 36775−81.
27. DeArmond, S. J., Sanchez, H., Yehiely, F., Qiu, Y., Ninchak-Casey, A., Daggett, V., Camerino, A. P., Cayetano, J., Rogers, M., Groth, D., Torchia, M., Tremblay, P., Scott, M. R., Cohen, F. E., and Prusiner, S. B. (1997) Selective neuronal targeting in prion disease, *Neuron 19*, 1337−48.
28. Neuendorf, E., Weber, A., Saalmueller, A., Schatzl, H., Reifenberg, K., Pfaff, E., and Groschup, M. H. (2004) Glycosylation deficiency at either one of the two glycan attachment sites of cellular prion protein preserves susceptibility to bovine spongiform encephalopathy and scrapie infections, *J. Biol. Chem. 279*, 53306−16.
29. Rogers, M., Taraboulos, A., Scott, M., Groth, D., and Prusiner, S. B. (1990) Intracellular accumulation of the cellular prion protein after mutagenesis of its Asn-linked glycosylation sites, *Glycobiology 1*, 101−9.
30. Lehmann, S., and Harris, D. A. (1997) Blockade of glycosylation promotes acquisition of scrapie-like properties by the prion protein in cultured cells, *J. Biol. Chem. 272*, 21479−87.
31. Muramoto, T., DeArmond, S. J., Scott, M., Telling, G. C., Cohen, F. E., and Prusiner, S. B. (1997) Heritable disorder resembling neuronal storage disease in mice expressing prion protein with deletion of an α-helix, *Nat. Med. 3*, 750−5.
32. Saborio, G. P., Permanne, B., and Soto, C. (2001) Sensitive detection of pathological prion protein by cyclic amplification of protein misfolding, *Nature 411*, 810−3.
33. Pan, K. M., Baldwin, M., Nguyen, J., Gasset, M., Serban, A., Groth, D., Mehlhorn, I., Huang, Z., Fletterick, R. J., Cohen, F. E., and Prusiner, S. B. (1993) Conversion of α-helices into β-sheets features in the formation of the scrapie prion proteins, *Proc. Natl. Acad. Sci. U.S.A. 90*, 10962−6.
34. Castilla, J., Saa, P., Hetz, C., and Soto, C. (2005) In vitro generation of infectious scrapie prions, *Cell 121*, 195−206.
35. Bocharova, O. V., Breydo, L., Parfenov, A. S., Salnikov, V. V., and Baskakov, I. V. (2005) In vitro conversion of full-length mammalian prion protein produces amyloid form with physical properties of PrP(Sc), *J. Mol. Biol. 346*, 645−59.
36. Riek, R., Hornemann, S., Wider, G., Glockshuber, R., and Wuthrich, K. (1997) NMR characterization of the full-length recombinant murine prion protein, mPrP(23-231), *FEBS Lett. 413*, 282−8.
37. Klohn, P. C., Stoltze, L., Flechsig, E., Enari, M., and Weissmann, C. (2003) A quantitative, highly sensitive cell-based infectivity assay for mouse scrapie prions, *Proc. Natl. Acad. Sci. U.S.A. 100*, 11666−71.
38. Deleault, N. R., Geoghegan, J. C., Nishina, K., Kascsak, R., Williamson, R. A., and Supattapone, S. (2005) Protease-resistant Prion Protein Amplification Reconstituted with Partially Purified Substrates and Synthetic Polyanions, *J. Biol. Chem. 280*, 26873−9.
39. Kocisko, D. A., Priola, S. A., Raymond, G. J., Chesebro, B., Lansbury, P. T., Jr., and Caughey, B. (1995) Species specificity in the cell-free conversion of prion protein to protease-resistant forms: A model for the scrapie species barrier, *Proc. Natl. Acad. Sci. U.S.A. 92*, 3923−7.
40. Silveira, J. R., Raymond, G. J., Hughson, A. G., Race, R. E., Sim, V. L., Hayes, S. F., and Caughey, B. (2005) The most infectious prion protein particles, *Nature 437*, 257−61.
41. Makarava, N., Bocharova, O. V., Salnikov, V. V., Breydo, L., Anderson, M., and Baskakov, I. V. (2006) Dichotomous versus palm-type mechanisms of lateral assembly of amyloid fibrils, *Protein Sci. 15*, 1334−41.
42. Priola, S. A., and Lawson, V. A. (2001) Glycosylation influences cross-species formation of protease-resistant prion protein, *EMBO J. 20*, 6692−9.
43. Rudd, P. M., Wormald, M. R., Wing, D. R., Prusiner, S. B., and Dwek, R. A. (2001) Prion glycoprotein: Structure, dynamics, and roles for the sugars, *Biochemistry 40*, 3759−66.

BI061526K